Nuclear Materials and Energy 12 (2017) 605–610

Contents lists available at ScienceDirect

Nuclear Materials and Energy

journal homepage: www.elsevier.com/locate/nme

TCV mirrors cleaned by plasma

L. Marot[a,*], S. Coda[b], S. Kajita[c], L. Moser[a], R. Steiner[a], E. Meyer[a]

[a] Department of Physics, University of Basel, Klingelbergstrasse 82, 4056 Basel, Switzerland
[b] EPFL-SPC, Station 13, CH-1015 Lausanne, Switzerland
[c] Institute of Materials and Systems for Sustainability, Nagoya University, Nagoya 464-8603, Japan

ARTICLE INFO

Article history:
Received 15 July 2016
Revised 2 June 2017
Accepted 12 June 2017
Available online 20 June 2017

ABSTRACT

Metallic mirrors exposed in TCV tokamak were cleaned by plasma in laboratory. A gold (Au) mirror was deposited with 185–285 nm of amorphous carbon (aC:D) film coming from the carbon tiles of TCV. Another molybdenum (Mo) mirror had a thicker deposit due to a different location within the tokamak. The thickness measurements were carried out using ellipsometry and the reflectivity measurements performed by spectrophotometry revealed a decrease of the specular reflectivity in the entire range (250–2500 nm) for the Mo mirror and specifically in the visible spectrum for the Au. Comparison of the simulated reflectivity using a refractive index of 1.5 and a Cauchy model for the aC:D gives good confidence on the estimated film thickness. Plasma cleaning using radio frequency directly applied to a metallic plate where the mirrors were fixed demonstrated the ability to remove the carbon deposits. A mixture of 50% hydrogen and 50% helium was used with a −200 V self-bias. Due to the low sputtering yield of He and the low chemical erosion of hydrogen leading to volatile molecules, 20 h of cleaning were needed for Au mirror and more than 60 h for Mo mirror. Recovery of the reflectivity was not complete for the Au mirror most likely due to damage of the surface during tokamak exposure (breakdown phenomena).

1. Introduction

One of the most crucial elements of optical diagnostics systems of ITER would be the so-called first mirrors (FMs), which will view the ITER plasma directly and will direct the signals into an optical labyrinth. Because of the different admixtures and ion fluxes at various locations of the machine, the mirrors will be subjected to mild or severe erosion and/or deposition. Performances of first mirrors have been addressed in several tokamaks and laboratory exposures [1]. Although passive mitigation techniques (specific duct geometry, shutters in front of the mirror, etc.) are predicted to reduce the amount of material deposited on FMs, suitable in situ cleaning solutions will be required to recover the FMs reflectance in ITER properly. Currently, plasma cleaning [2–4] and laser cleaning [5,6] or even combined [7] are considered the most promising solutions.

This work presents the results of plasma cleaning of two metallic coated mirrors [8] used in Tokamak à Configuration Variable (TCV) [9] for CO_2 laser transmission for fluctuation measurements using interferometric techniques. Characterisations of the mirrors were performed after TCV exposure, and the deposited carbon film thickness was calculated by ellipsometry. RF plasma cleaning was then performed in laboratory leading to the recovery of the reflectivity.

2. Experimental

Two mirrors used in TCV tokamak for CO_2 laser transmission for fluctuation measurements using the phase-contrast technique [10] (Fig. 1a) were used for plasma cleaning test in laboratory. Mirrors were new and in a pristine state before exposure. These flat elliptical mirrors, with linear dimensions exceeding 100 mm, were made of fused silica coated with Mo or Au (100–200 nm) reflecting layers protected by a 10–20 nm SiO (Fig. 1b). Fig. 1a) displayed an extreme configuration for the photography but in reality, the mirror assembly is recessed into the port at all times. The Mo- or Au-coated mirrors were in the vessel for an estimated ~6500 and ~5500 plasma shots, respectively (average shot length 1.7 s), and were also exposed to 5 min He glow discharges (−500 V DC) performed routinely between plasma shots. The strategy for these mirrors was to keep the reflective coating electrically floating, by leaving the clamping points uncoated to prevent ion bombardment during glow discharge cleaning. This was the case for the Mo mirror while unfortunately for the Au mirror the coating

* Corresponding author.
E-mail address: laurent.marot@unibas.ch (L. Marot).

http://dx.doi.org/10.1016/j.nme.2017.06.006

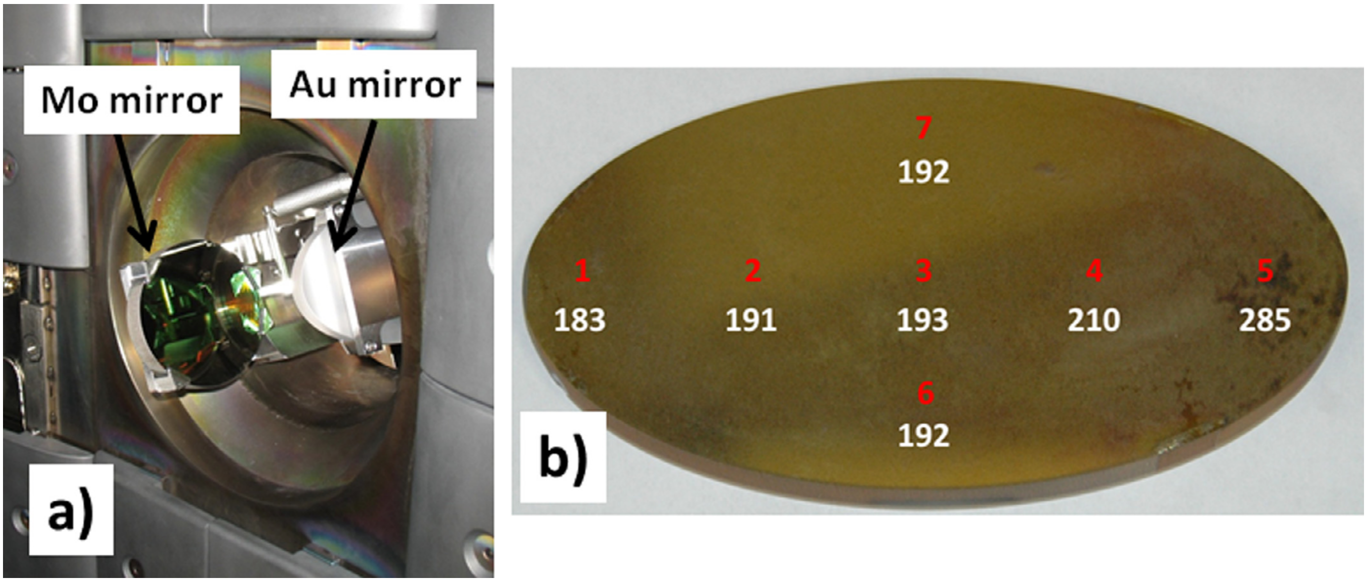

Fig. 1. a) Mo and Au mirrors mounted in TCV. The outermost tip of the Mo mirror generally sits just behind the level of the graphite tile surface. b) Image of the gold mirror, position of measurements on this mirror are in red and the film thickness calculated by ellipsometry is below. Position 5 is the closest point to the TCV plasma. (For interpretation of the references to colour in this figure legend, the reader is referred to the web version of this article.)

was still present below the clamp. The plasmas were fully ionized, high-temperature (several keV) deuterium plasmas. The mirrors were well recessed not only outside of the region of closed fluxed surfaces but also outside the surface of the plasma-facing graphite tiles. Most of the bombardment during plasma shots can be expected to come from charge-exchange neutrals escaping the core, whereas during glow discharge, sputtering it is from accelerated ions - but there is evidence to indicate that this is a minor effect. Plasma cleaning using radio frequency (RF 13.56 MHz) directly applied to a metallic plate (RF capacitively coupled discharge) as classically used by Moser et al. [3] on which the fused silica mirrors were fixed, were carried out using a mixture of 50% hydrogen (H_2) and 50% helium (He) at 1×10^{-2} mbar and 110 W leading to −200 V self-bias. Due to the asymmetry between the powered and grounded areas, a negative DC component (called self-bias) is created on the electrode/mirror, accelerating the plasma ions towards the mirror's surface (H^+ and/or He^+). As the fused silica mirror is fixed on a metallic electrode and covers only 13% of its surface, the self-bias displayed by the generator is assumed to be equal to the self-bias of the insulating surface. No magnetic field was used during plasma cleaning. Due to the low sputtering yield of He and the low chemical erosion of hydrogen leading to volatile molecules, 20 h of cleaning were needed for the Au mirror and more than 60 h for the Mo mirror. Taking into account the ionization potentials difference between H_2 and He, the He ion flux can be lower as the H_2 one.

Total and diffuse reflectivity measurements were carried out with a Varian Cary 5 spectrophotometer equipped with an 110 mm diameter integrating sphere under nearly normal incidence (3°20') in the wavelength range of 250–2500 nm. Spectroscopic ellipsometry measurements were done in variable angle configuration using a Sentech 850 device at incident angles of 4°, 55 and 65° for a wavelength range of 300–2300 nm. The morphology of the mirror was investigated by top view scanning electron microscopy (SEM) (Hitachi S-4800 field emission at 5 kV).

3. Results

As TCV was composed of graphite plasma-facing materials and as deuterium was the main plasma fuel, we can assume that the deposited layer was mainly composed of carbon and deuterium. Chemicals analyses of the surface using X-Ray Photoelectron Spectroscopy (not shown here) revealed only carbon and oxygen. The optical properties (refractive index n and extinction coefficient k) of a-C:D film can be accurately described with a Cauchy relation where n_i, and k_i are fitting parameters [11]. The films are considered as homogeneously deposited on a semi-infinite substrate, and the roughness of both the film and the substrate are neglected. Film thickness was calculated and displayed in Fig. 1b), 100 nm thickness difference is measured along the position to the plasma, and vertically no change appeared. The n (at 632.5 nm) varied from 1.48 to 1.56 for all points and k was calculated to be zero. This revealed a soft hydrocarbon film typical for mirrors exposed in TCV [12] and resembled T-10 tokamak (Kurchatov Institute) cleaning discharge films on mirrors [13]. The reflectivity calculated using the model: air, our Cauchy film, SiO film (10 nm) and an Au layer using the Palik constant is plotted in Fig. 2. In the same figure, the

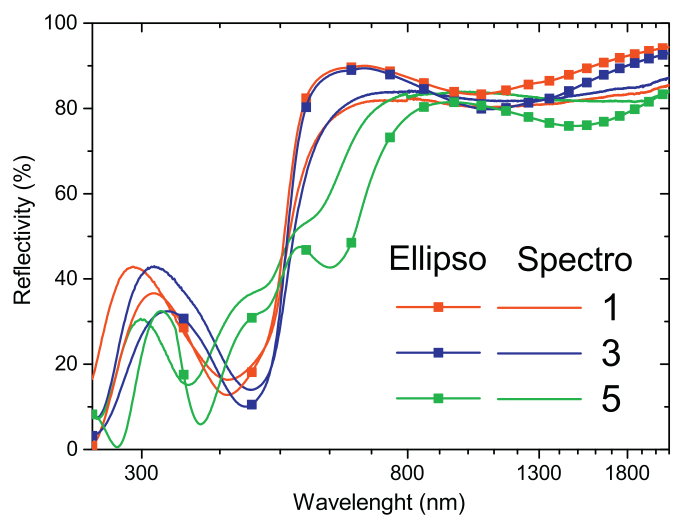

Fig. 2. Calculated reflectivity using the Cauchy model and the reflectivity measured using a spectrophotometer for the Au mirror, at the positions displayed in Fig. 1b). The X axis is on a log scale.

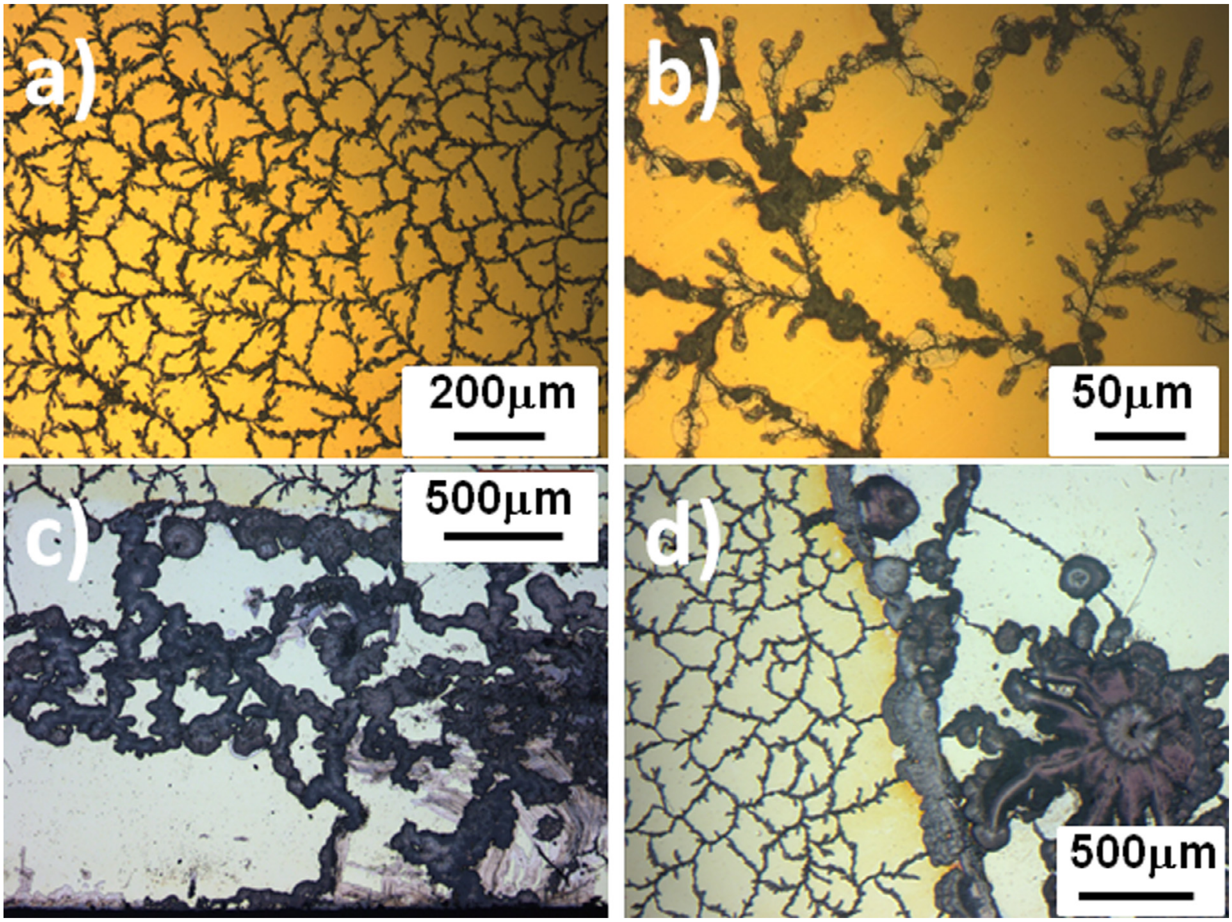

Fig. 3. a) and b) are optical images of the Au mirror after TCV exposure in the centre of the mirror. c) and d) are optical images of the Au mirror below the clamping part (Fig. 1a). Below the clamp wide arcing trails are present and at the limit of the clamp typical breakdown phenomena are observed everywhere.

reflectivity measured with the spectrophotometer for the same position is also plotted. The relatively good agreement between both methods validates our model with the calculated film thickness.

Optical images were also recorded after TCV exposure and are displayed in Fig. 3a) and b) for the Au mirror. The entire mirror is covered with a network like structure damage. It is likely that the damage was caused by serious breakdown phenomena occurring on the surface. The trail bifurcated frequently and, in Fig. 3b), common electrical treeing phenomena can be identified. It is likely that melting/evaporation of the materials occurred and trails were formed while breakdown spots ran on the surface. On the dark part of the trail, the Au layer is likely to have been fully removed, while on the bright part of the trail, only the insulating coating and part of Au layer were melted and removed. The observed trail width was ∼10 μm, which is consistent with the typical width of arc trails [14]. In contrast with these short bifurcated trails, major arc trails (Fig. 3c) were observed below the four clamps (Fig. 1a) major arc trails (Fig. 3c) with a width of 60–100 μm. In this case, the grounded clamp was directly on the mirror. As described in Schwirzke's model [15], a unipolar arc can be sustained by forming a current loop locally. We can suppose that the arc trails shown in Fig. 3a) and b) covering the entire mirror correspond to the cathodic and Fig. 3c) and d) locating below the clamps to anodic footprints. In Fig. 3d) we identified an arc crater [15]. Moreover, we cannot completely dismiss that traces overlapped from different occasions.

It is known that arc trails usually have fractal features [14]. To measure the fractal dimension of the trail, a box counting method was applied to the trail. In this approach [17], the image (Fig. 3a)

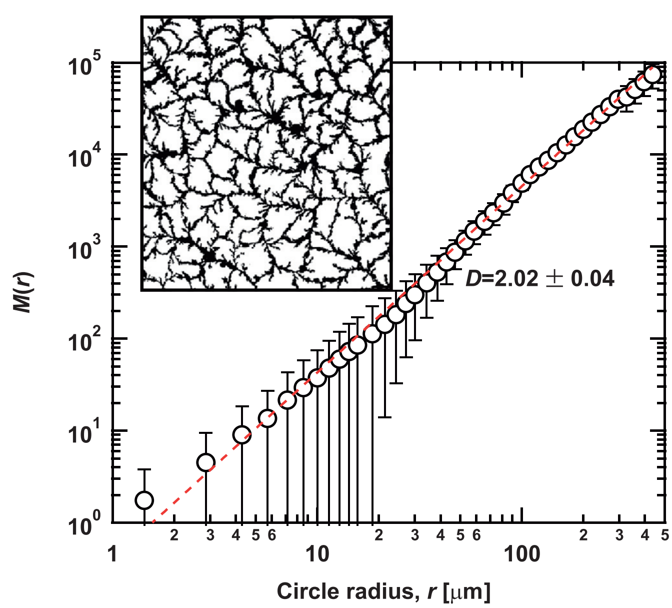

Fig. 4. The number of dots in a circle *M(r)* is plotted on a logarithmic scale as a function of the radius r_{box} for the images shown in Fig. 3.

was digitized first and then the number of black dots in a circle, *M(r)*, was counted for varying circle radius, *r*. Fig. 4 shows the function *M(r)* using the digitized image shown in the inset. It is seen that a power law relation between *M(r)* and *r* was identi-

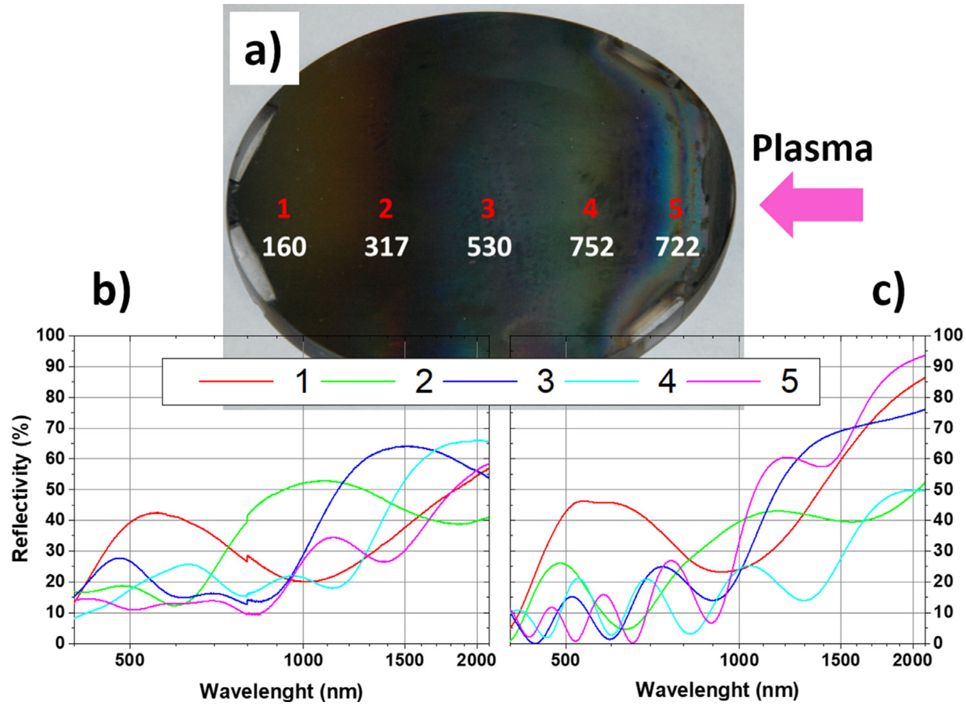

Fig. 5. a) Mo mirror after TCV exposure: the measurements positions on this mirror are in red and the film thickness calculated by ellipsometry is below, b) reflectivity measured by spectrophotometry and c) calculated by ellipsometry. (For interpretation of the references to colour in this figure legend, the reader is referred to the web version of this article.)

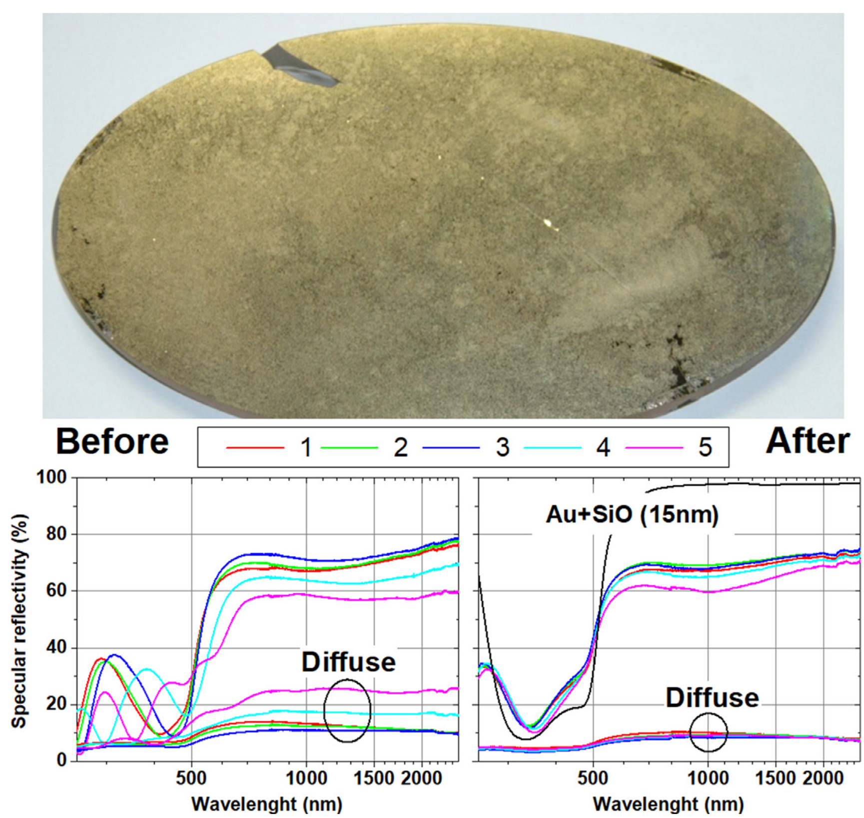

Fig. 6. Optical image of the Au mirror after plasma cleaning. Specular and diffuse reflectivity of the Au mirror measured before and after plasma cleaning. Au reflectivity using Palik optical constant is plotted as reference.

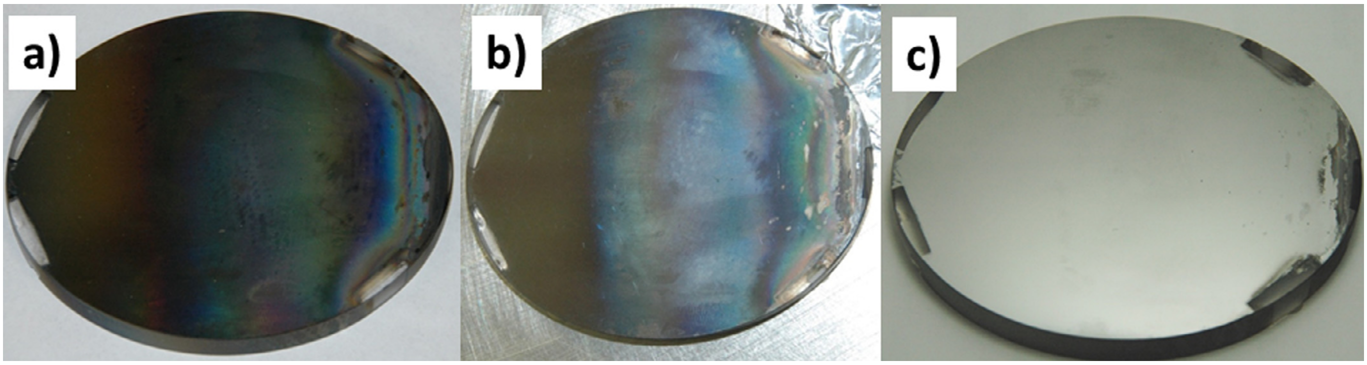

Fig. 7. Optical images of the Mo mirror before plasma cleaning a), after 13h40 at −200 V b) and after 60h40. The last plasma cleaning was with −250 V bias.

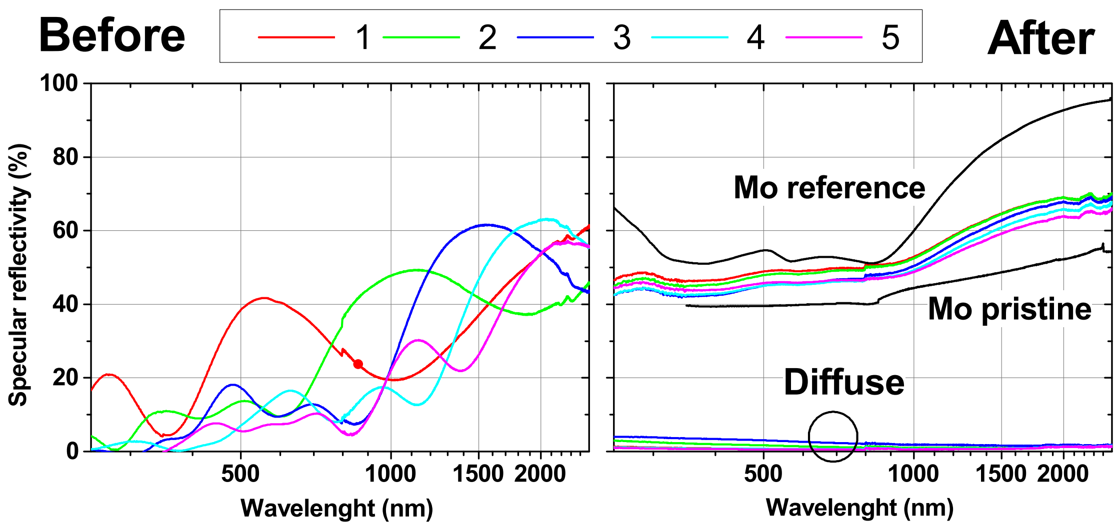

Fig. 8. Specular reflectivity of the Mo mirror measured before and after plasma cleaning. Mo reflectivity using Palik optical constant as well as the measured Mo pristine from the manufacturer are plotted as references.

fied on the scale from 1 to 500 µm. From the slope of the data, we deduced that the fractal (box counting) dimension, D, was ~2.02 ± 0.04. Previously, it was found that D of arc trails decreases with increasing magnetic field strength from two to unity. This means that the motion of arc spots changes from random (D~2.0) to linear (D~1.0) for increasing magnetic field strength. As reported by Kajita et al. [17], a variation of the magnetic field from 0.02 to 0.2 T induced changes of D from 2 to 1.5, respectively. In the presence of magnetic fields, the trail moves across the material in the direction perpendicular to the magnetic field [18]. This effect is known as retrograde motion and it produces characteristic dendrite-like tracks as explained by B. Jüttner et al. [19]. Based on this analogy, it is suggested that breakdown in Fig. 3 occurred without the existence of magnetic field. In other words, it would have taken place during glow discharge cleaning, which is performed in TCV primarily with a DC voltage of 500 V. However, when we focus on the bifurcated position of the trail (Fig. 3(c)), it is seen that the trail spreads to various direction like treeing. In the case of a strong magnetic field, bifurcated spots should also move in the same direction, as was shown in the case of JT-60U [16]. Thus, it is likely that the breakdown was initiated without magnetic field.

Previously, fatal damages were also observed on a diagnostic mirror for Thomson scattering diagnostics in JT-60U [20]. In the JT-60U case, the mirror was located outside the vacuum chamber. Since the mirror was electrically isolated, charge up processes are necessary to initiate and sustain the breakdown, and possible charge up mechanism on the surface was high energy photons or radiations in the JT-60U case. In the present case, charge up can occur by the bombardment of charged particles. In the present case, as the Au layer of the mirror was grounded and not floating as it should, the SiO surface can charge up (due to the ion bombardment issued from the GDC) up to the point where the charges could be accumulated in the insulating layer and the field strength would exceed to initiate dielectric breakdown. A breakthrough can then occur from SiO to Au leading to these typical electrical treeing phenomena. This was especially the case for the Au mirror; the clamping part was not removed and below was either not damage coating or large arcing in reference 18. The breakdown phenomena (Fig. 3) which covered the entire mirror started at the limit of the clamps. The mirror was probably connected to the ground and with the SiO/Au/SiO during GDC, the SiO was charging up and with this 500 V a breakthrough SiO occurred to the Au with leading to these electrical treeing phenomena.

The Mo mirror was also measured in the same way: a higher thickness gradient (> 560 nm) between the closest position to the plasma and the back of the mirror was calculated (Fig. 5a). The thicker carbon film can be explained by the longer exposure time in TCV and also the position with respect to the plasma. The reflectivity measured by the spectrophotometer and the one calculated by the Cauchy model as previously explained are not entirely the same especially in the near infrared region (Fig. 5). Optical images after TCV exposure do not show the electrical treeing phenomena observed in Fig 3.

A 20 h plasma cleaning was performed on the Au mirror using a H_2/He gas mixture for a self-bias of −200 V. The specular reflectivity (total minus diffuse) is plotted in Fig. 6 before and after cleaning. No measurement of the pristine Au mirror is available so in Fig. 6 (After) is displayed the reflectivity of Au with 15 nm SiO calculated using the optical constant of both materials. Even though the reflectivity after cleaning is lower than the reference, the strong absorption at 350 nm is reproduced by the calculated reflectivity. An important point is the diffuse reflectivity after cleaning which is 10% higher as plotted in Fig. 6 and gives this visual milky aspect after cleaning (Fig. 6). After TCV exposure the diffuse reflectivity was higher than 25% in the range 800–2500 nm (Fig. 6). After plasma cleaning, SEM or optical images (not shown here) revealed the same unchanged pattern. Removal of the carbon film by plasma cleaning did not change this phenomenon resulting in an always high diffuse reflectivity.

Optical images of the Mo mirror before plasma cleaning a), after 13h40 at −200 V b) and after 60h40 are displayed in Fig. 7. The last plasma cleaning cycle was with −250 V (169 W RF power). Visually after the first cleaning, the interference fringes changed due to film thickness removal and later the mirror had a metallic aspect. Recovery of the reflectivity after the last cleaning is shown in Fig. 8, the pristine reflectivity measured by the manufacturer is also plotted. In comparison, the Mo reflectivity calculated with the Palik optical constant is displayed too. The diffuse reflectivity after plasma cleaning was below 4% for the entire range. SEM images (not shown here) after plasma cleaning revealed that the top silicon oxide layer had peeled off. However, the diffuse reflectivity was really low as this typical electrical treeing phenomenon was not observed for this mirror on floating potential.

6. Concluding remarks

Plasma cleaning using RF directly applied to a metallic plate to which the fused silica mirrors were attached demonstrated the ability to remove the carbon deposits after TCV exposure. Reflectivity measurements with a spectrophotometer compared to the simulated reflectivity using a refractive index of 1.5 and a Cauchy model for the aC:D gives good confidence in the estimated film thickness. Due to the low sputtering yield of He and the low chemical erosion of H leading to volatile molecules, a long cleaning time was required with a self-bias of −200 V. Recovery of the reflectivity was not complete for the Au mirror mostly due to damage to the surface by tokamak exposure i.e. breakdown phenomena typical for electrical treeing. A fractal dimension of 2 was calculated for these breakdown phenomena which is typical for the random motion of arc spot.

Acknowledgements

The authors would like to thank the Swiss Federal Office of Energy (grant no.) SI/500044-04 and the Federal Office for Education and Science (grant no.) 1315000002 for their financial support. This work was also supported by the Swiss National Foundation (SNF) and the Swiss Nanoscience Institute (SNI).

References

[1] V.S. Voitsenya, A.F. Bardamid, A.J.H. Donné, Experimental simulation of the behaviour of diagnostic first mirrors fabricated of different metals for ITER conditions, Open Phys. J. 3 (2016) 23–54, doi:10.2174/187484300160301002.
[2] A.G. Razdobarin, A.M. Dmitriev, A.N. Bazhenov, I.M. Bukreev, M.M. Kochergin, A.N. Koval, G.S. Kurskiev, A.E. Litvinov, S.V. Masyukevich, E.E. Mukhin, D.S. Samsonov, V.V. Semenov, S.Y. Tolstyakov, P. Andrew, V.L. Bukhovets, A.E. Gorodetsky, A.V. Markin, A.P. Zakharov, R.K. Zalavutdinov, P.V. Chernakov, T.V. Chernoizumskaya, A.A. Kobelev, I.V. Miroshnikov, A.S. Smirnov, RF discharge for *in situ* mirror surface recovery in ITER, Nucl. Fusion 55 (2015) 93022, doi:10.1088/0029-5515/55/9/093022.
[3] L. Moser, R. Steiner, F. Leipold, R. Reichle, L. Marot, E. Meyer, Plasma cleaning of ITER First Mirrors in magnetic field, J. Nucl. Mater. 463 (2015) 940–943, doi:10.1016/j.jnucmat.2014.11.087.
[4] L. Moser, L. Marot, B. Eren, R. Steiner, D. Mathys, F. Leipold, R. Reichle, E. Meyer, Towards plasma cleaning of ITER first mirrors, Nucl. Fusion 55 (2015) 63020, doi:10.1088/0029-5515/55/6/063020.
[5] A. Maffini, A. Uccello, D. Dellasega, V. Russo, S. Perissinotto, M. Passoni, Laser cleaning of diagnostic mirrors from tokamak-like carbon contaminants, J. Nucl. Mater. 463 (2015) 944–947, doi:10.1016/j.jnucmat.2014.10.016.
[6] M. Wisse, L. Marot, A. Widdowson, M. Rubel, D. Ivanova, P. Petersson, R.P. Doerner, M.J. Baldwin, J. Likonen, E. Alves, A. Hakola, S. Koivuranta, R. Steiner, E. Meyer, Laser-assisted cleaning of beryllium-containing mirror samples from JET and PISCES-B, Fusion Eng. Des. 89 (2014) 122–130, doi:10.1016/j.fusengdes.2014.01.042.
[7] A. Maffini, L. Moser, L. Marot, R. Steiner, D. Dellasega, A. Uccello, E. Meyer, M. Passoni, *In situ* cleaning of diagnostic first mirrors: an experimental comparison between plasma and laser cleaning in ITER-relevant conditions, Nucl. Fusion 57 (2017) 46014, doi:10.1088/1741-4326/aa5d05.
[8] L. Marot, G. Arnoux, A. Huber, V. Huber, P. Mertens, G. Sergienko, E. Meyer, J.E.T. Contributors, Optical coatings as mirrors for optical diagnostics, J. Coat. Sci. Technol. 2 (2016) 72–78, doi:10.6000/2369-3355.2015.02.03.1.
[9] S. Coda, TCV Team, The science program of the TCV tokamak: exploring fusion reactor and power plant concepts, Nucl. Fusion 55 (2015) 104004, doi:10.1088/0029-5515/55/10/104004.
[10] A. Marinoni, S. Coda, R. Chavan, G. Pochon, Design of a tangential phase contrast imaging diagnostic for the TCV tokamak, Rev. Sci. Instrum. 77 (2006) 10E929, doi:10.1063/1.2222333.
[11] J. Rapp, G.J. van Rooij, A. Litnovsky, L. Marot, G. De Temmerman, J. Westerhout, E. Zoethout, Temperature effect on hydrocarbon deposition on molybdenum mirrors under ITER-relevant long-term plasma operation, Phys. Scr. T138 (2009) 14067, doi:10.1088/0031-8949/2009/T138/014067.
[12] G. De Temmerman, R.A. Pitts, Substrate-dependent deposition efficiency on mirrors exposed in the TCV divertor, Fusion Eng. Des. 83 (2008) 30–38, doi:10.1016/j.fusengdes.2007.04.044.
[13] I. Arkhipov, N. Klimov, N. Svechnikov, S. Grashin, K. Vukolov, V. Budaev, K. Maslakov, V. Stankevich, A. Zhitlukhin, D. Kovalenko, V. Podkovyrov, Experimental study of contamination and cleaning of in-vessel mirrors for ITER optical diagnostics on T-10 and QSPA-T facilities, J. Nucl. Mater. 438 (2013) S1160–S1163, doi:10.1016/j.jnucmat.2013.01.256.
[14] A. Anders, Cathodic Arcs: From Fractal Spots to Energetic Condensation, Springer, New York, 2008.
[15] F.R. Schwirzke, Vacuum breakdown on metal surfaces, IEEE Trans. Plasma Sci. 19 (1991) 690–696, doi:10.1109/27.108400.
[16] S. Kajita, M. Fukumoto, M. Tokitani, T. Nakano, Y. Noiri, N. Ohno, S. Masuzaki, S. Takamura, N. Yoshida, Y. Ueda, Impact of arcing on carbon and tungsten: from the observations in JT-60U, LHD and NAGDIS-II, Nucl. Fusion 53 (2013) 53013, doi:10.1088/0029-5515/53/5/053013.
[17] S. Kajita, S. Takamura, N. Ohno, Motion of unipolar arc spots ignited on a nanostructured tungsten surface, Plasma Phys. Control. Fusion 53 (2011) 74002, doi:10.1088/0741-3335/53/7/074002.
[18] A. Garcia-Carrasco, P. Petersson, M. Rubel, A. Widdowson, E. Fortuna-Zalesna, S. Jachmich, M. Brix, L. Marot, Plasma impact on diagnostic mirrors in JET, Nucl. Mater. Energy (2017), doi:10.1016/j.nme.2016.12.032.
[19] B. Jüttner, I. Kleberg, The retrograde motion of arc cathode spots in vacuum, J. Phys. Appl. Phys. 33 (2000) 2025–2036, doi:10.1088/0022-3727/33/16/315.
[20] S. Kajita, T. Hatae, T. Sakuma, S. Takamura, N. Ohno, K. Itami, Fatal damages due to breakdown on a diagnostic mirror located outside the vacuum vessel in JT-60U, Plasma Fusion Res. 7 (2012) 2405121–2405121, doi:10.1585/pfr.7.2405121.